doi.org/10.36721/PJPS.2026.39.2.REG.14740.1

Lauric acid mitigates doxorubicin-induced cardiotoxicity in rats: Modulation of oxidative stress and inflammation via NF-κB p65 attenuation

Samreen Aziz[1,2]*, Humera Khatoon[1], Aisha Aziz[1], Muhammad Imran[2] and Azfar Athar Ishaqui[3]
[1]Department of Pharmacology, Faculty of Pharmacy, Jinnah University for Women, Karachi, Pakistan
[2]Faculty of Pharmacy, Iqra University - North Campus, Karachi, Pakistan
[3]Department of Clinical Pharmacy, College of Pharmacy, King Khalid University, Abha, Saudi Arabia

Abstract: **Background**: Cardiotoxic effects of doxorubicin (DOX) have been reported in cancer patients, which mainly stem from the production of reactive oxygen species (ROS). This oxidative damage contributes to myocardial injury, inflammation, and altered cardiac function. Lauric acid (LA) is a medium-chain saturated fatty acid present in coconut oil and is known for its antioxidant properties, making it a potential cardioprotective candidate against DOX-induced toxicity. **Objectives**: The present study was conducted to evaluate the cardioprotective effects of LA in a DOX-induced cardiotoxicity model by assessing biochemical, hematological, oxidative stress, histological, and molecular parameters in Wistar rats. **Methods**: Wistar rats were divided into four groups (n = 6): control (Tween 20), LA (500 mg/kg), DOX (15 mg/kg) and LA + DOX groups. The rats were sacrificed and evaluated for hematological indices, lipid profile and cardiac biomarkers, including CK-MB, cardiac troponin I (cTnI) and LDH. Cardiac tissue was analyzed for MDA, CAT, SOD, histopathological assessment, gene expression (NF-κB p65, IL-6 and TNF-α) and cytokine levels (IL-6 and TNF-α) after the 14-day study period. Additional comparative evaluation between DOX and LA + DOX groups was performed to determine the extent of cardioprotection. **Results**: The DOX reduced the body weight of rats, dysregulated hematological and lipid profiles and upregulated cardiac markers in serum. It also increased MDA levels, depleted CAT and SOD levels, altered cardiac cell histoarchitecture and elevated the gene and protein expressions of the cytokines. LA mitigated DOX-mediated cardiotoxicity by reducing oxidative stress and inflammation. LA also improved biochemical values, preserved myocardial structure and restored the antioxidant status compared to the DOX group. **Conclusion**: In conclusion, LA treatment protects the cardiac tissue against DOX-induced cardiotoxicity, as evidenced by its antioxidant and anti-inflammatory potential, supporting its possible therapeutic role.

Keywords: Doxorubicin-induced cardiotoxicity; Lauric acid; NF-κB signaling pathway; Oxidative stress; Pro-inflammatory cytokines

Submitted on 13-06-2025 – Revised on 09-07-2025 – Accepted on 11-07-2025

INTRODUCTION

DOX has been used in combination with other chemotherapeutic drugs or alone as a first line of treatment for several metastatic or solid tumors (Sritharan & Sivalingam, 2021), including childhood solid tumors, acute leukemia, breast cancer, Hodgkin's disease, non-Hodgkin lymphomas and soft tissue sarcomas. (Meredith & Dass, 2016). Despite its effectiveness in cancer treatment, DOX is non-specific to cancer cells and, hence, poses toxic effects in the body, which limits its use to a great extent. The heart, brain, kidneys and liver are among the primary organs affected by DOX-induced toxicity, the consequences of which may unfold over many years (Pugazhendhi *et al*., 2018). The clinical presentation of DOX-associated cardiac dysfunction includes a wide range of symptoms, from cardiac arrhythmias to congestive heart failure (Mitry & Edwards, 2016). There is substantial evidence to report the involvement of oxidative stress, mitochondrial dysfunction and inflammation in DOX-induced cardiotoxicity. (Linders *et al*., 2024). In DOX-mediated oxidative stress, excessive formation of reactive oxygen species (ROS) occurs through iron-mediated and mitochondrial redox cycling, as illustrated in fig. 1. Iron-dependent redox cycling results in oxidative injury to nucleic acids and proteins, culminating in mitochondrial collapse and apoptosis (Aryal & Rao, 2016). Mitochondria are densely packed in the cardiomyocyte cytoplasm to support their high metabolic activity (Linders *et al*., 2024). Cardiolipin, a phospholipid exclusive to the inner mitochondrial membrane, is vital for regulating mitochondrial energy function and membrane potential, which facilitates the accumulation of DOX in mitochondria due to its high binding affinity for the drug. (Aryal & Rao, 2016). This localization facilitates DOX's interaction with the electron transport chain (ETC), particularly Complex I [Nicotinamide adenine dinucleotide hydride dehydrogenase (NADH dehydrogenase)], which reduces DOX into a semiquinone anion radical and leads to the formation of superoxide ion ($O_2^{\bullet -}$) after reacting with molecular oxygen. Therefore, the ensuing leakage of electrons contributes to the generation of ROS, resulting in oxidative stress (Angsutararux *et al*., 2015). ROS generation is manifested as lipid peroxidation and mitochondrial and cardiac cell membrane damage (Shi *et*

**Corresponding author:* e-mail: samreen.fareed1987@gmail.com

al., 2023). Beyond oxidative damage, inflammation is considered a key pathological factor in DOX-induced cardiotoxicity. As a consequence of oxidative stress, an inflammatory response is initiated through the activation of the Nuclear factor kappa B (NF-κB) signaling pathway, which is essential in modulating immune activity, cell survival and the inflammatory response. This widely expressed transcription factor drives the upregulation of several inflammatory cytokines, mainly interleukin-6 (IL-6) and tissue necrosis factor-alpha (TNF-α), which serve as indicators of inflammation associated with DOX intoxication (El-Agamy *et al*., 2018). Therapeutic strategies targeting oxidative stress and inflammation are effective in mitigating DOX-mediated cardiotoxicity (Alharbi *et al*., 2023; Hany *et al*., 2022). LA is a medium-chain 12-carbon saturated fatty acid, a significant constituent of coconut and palm kernel oil (Akula *et al*., 2021; Silalahi *et al*., 2018; Türkmen & Koçer, 2021) and has gained recognition due to its wide range of biological actions, including antioxidant, anti-inflammatory and antimicrobial effects(Anuar *et al*., 2023b; Mustafa *et al*., 2023; Nitbani *et al*., 2022). The medium chain length provides LA with a competitive advantage over long chain fatty acids in its metabolism, by which medium chain fatty acids (MCFA) enter the liver via the hepatic portal vein (Nakajima & Kunugi, 2020) and are utilized into energy and the energy metabolites like ketone bodies via a carnitine-independent pathway in mitochondria rather than being stored in adipose tissues (Nonaka *et al*., 2016). Recent studies clarified the effectiveness of LA in cardiac health. A study revealed that LA significantly reduced blood pressure in hypertensive rats and possessed vasorelaxant effects by lowering oxidative stress (Alves *et al*., 2017). Furthermore, the anti-inflammatory effect of LA was observed, as it lowered the concentration of the pro-inflammatory cytokine TNF-α in the lungs of diabetic rats, suggesting the alleviation of inflammation (Dubo *et al.,* 2019). While the antioxidant and anti-inflammatory effects of LA have been explored in various disease models, its role in protecting against DOX-induced cardiac injury has thus far remained elusive. Given the commonality in molecular signaling routes affected by DOX toxicity and those regulated by LA, there is a compelling rationale to assess the cardioprotective potential of LA. Therefore, our study aimed to explore the cardioprotective effects of LA in DOX-mediated cardiotoxicity *in vivo*, with a focus on its antioxidant and anti-inflammatory mechanisms.

MATERIALS AND METHODS

Drugs, chemicals and reagents

LA ($C_{12}H_{24}O_2$, Cas No. 143-07-7), 2-thiobarbituric acid (TBA), trichloroacetic acid (TCA) and malondialdehyde (MDA) were purchased from Sigma-Aldrich (St. Louis, MO, USA). Doxorubicin Hydrochloride (50 mg/25 ml) was obtained from Himmel Pharmaceuticals (Pvt) Ltd. Sandwich ELISA kits were purchased from Cloud-Clone Corp. (Wuhan, China) for IL-6 (Cat: SEA079Ra) and TNF-α (Cat: SEA133Ra). Micro-method assay kits for antioxidant enzymes superoxide dismutase (SOD: Ref D799594-0100) and Catalase (CAT: Ref D799598-0100) were acquired from Sangon Biotech (Shanghai, China). All other chemicals utilized in the study were of analytical grade.

Experimental animals

Adult Wistar rats of either sex (9-10 weeks old, weighing 200-250 grams) were selected for the study. Animals were bred at the Department of Pharmacology, Faculty of Pharmacy, Jinnah University for Women, Karachi, Pakistan. The animals were housed under controlled environmental conditions (temperature: 25 ± 5°C, humidity: 50 ± 10%, 12-hour light/dark cycle) with free access to food and water. Behavioral monitoring of animals was conducted one week before dosing, including observation of eating, defecating and urinating patterns, as well as behavioral changes such as depression and drowsiness. Animal selection was done randomly, using a computer-generated random number sequence and divided into a control group (n = 6) and a treatment group (n = 6). The sample size was chosen based on standard practices used in similar studies reported in the literature (Mahdizadeh *et al*., 2025).

Experimental design

The experimental design is illustrated in fig. 2. Twenty-four animals were divided into four groups (n = 6). The dose of LA (500 mg/kg) used in this study was selected based on preliminary dose-response testing in the DOX-induced cardiotoxicity model. In this pilot phase, rats received LA at 250, 500, 1000, and 2000 mg/kg with DOX to find the best cardioprotective dose (Supplementary Figures S1–S4). The best biochemical results were obtained with 500 mg/kg, thus it was used in following tests. The control group was administered Tween 20 once daily via intragastric intubation, which served as a vehicle for LA. The LA group received a 500 mg/kg dose once daily via intragastric intubation. The LA-only group was included to assess any intrinsic effects of LA on cardiac and biochemical parameters in the absence of DOX. The DOX group received a 15mg/kg cumulative dose (Warpe *et al*., 2015) via intraperitoneal (i.p) injection on the 10^{th} day. LA + DOX group was administered LA (500 mg/ kg) once daily for 14 days and DOX (15mg/ kg) was given on the 10^{th} day of the study. After the 14-day experimental period, all animals were fasted for 16 hours, a 300 mg/ kg (i.p) injection of chloral hydrate was administered for euthanizing animals and blood was collected via cardiac puncture. For assessing hematological indices, blood was collected in anticoagulant tubes. For serum separation, the blood samples were centrifuged at 3000 rpm for 10 minutes. All serum samples were collected and marked in Eppendorf tubes and kept in the -40 ◦C freezer before they were tested for biochemical analysis using specific diagnostic kits.

Determination of body and heart weight

All experimental animals' body weights were recorded at the start (day 0) and the end of the study (day 14). After euthanizing the rats, the heart was removed, the heart weight was measured and the relative heart weight to body weight percentage was calculated. The comparative analysis evaluated the differences between the control and test groups.

Assessment of hematological and biochemical parameters

Hematological parameters, including hemoglobin (Hb), hematocrit, red blood cell (RBC), white blood cell (WBC), differential count and platelet count, were evaluated in blood samples using an automatic hematology analyzer (HumaCount 80TS, HUMAN Diagnostics Worldwide, Germany). Semi-automatic HumaLyzer 3500 (HUMAN Diagnostics Worldwide, Germany) was used to determine serum total cholesterol (TC), triglycerides (TG), low-density lipoprotein (LDL) and high-density lipoprotein (HDL) based on the enzymatic colorimetric method and using diagnostic kits supplied by (HUMAN Diagnostics Worldwide, Wiesbaden, Germany). The levels of serum creatine phosphokinase-MB (CK-MB), cTnI and lactate dehydrogenase (LDH) were measured to confirm injury in myocardial tissue using their specific reagent kits (Biosystems S.A, Spain) as per the manufacturer's manual guide using a semi-automatic analyzer (BioSystems BTS-350® biochemistry, Biosystems S.A, Spain).

Estimation of oxidative stress and antioxidant enzyme activity

Lipid peroxidation in cardiac tissue was determined with Thiobarbituric Acid Reactive Substances (TBARS) assay by measuring the levels of its byproduct, MDA, expressed as nmol/ milligram of tissue. 100 mg of cardiac tissue was homogenized using 1mL phosphate-buffered saline (PBS, pH 7.4) to collect the supernatant by centrifugation at 10,000 g for 15 minutes. Protein denaturation was performed by centrifugation and forming precipitates using 20% TCA. 0.33% TBA was added to the supernatant and boiled for 1 hour at 95 °C to allow MDA-TBA reaction. After cooling down, the samples were extracted with butanol to amplify the pink color intensity. The samples were finally centrifuged to measure absorbance using a microplate photometer (Thermo Scientific Multiskan FC, USA) at 532 nm. 1000 µM stock solution of MDA was prepared to make dilutions over the 0-40 nmol/mL range to quantify MDA levels in samples using a standard curve linear equation (Naderi *et al*., 2023). Levels of CAT and SOD were assessed in cardiac tissue as a measure of antioxidant enzyme status in animal groups by employing commercial assay kits and following the manufacturer's protocol. The activity of CAT was determined by a micro method based on H_2O_2 decomposition at 240 nm using a UV-Vis spectrophotometer (Shimadzu UV-1800, Shimadzu Corporation, Kyoto, Japan). The activity of CAT was analyzed by measuring the drop in absorbance value at 240 nm over time and calculating the rate of change in absorbance. The enzymatic activity of SOD was detected with the principle of the xanthine-xanthine oxidase reaction system to trigger superoxide anions (O_2-) generation that forms blue formazan by reducing nitroblue tetrazolium (NBT). SOD inhibits the formation of formazan by neutralizing O_2- and a decrease in absorbance value at 560 nm was measured.

Histopathological examination

Hematoxylin and eosin (H&E) staining was employed to evaluate the histological architecture of the cardiac tissues of all animal groups. After completing the fixation of the tissue samples in 10% formalin, a graded series of ethanol dehydration was processed before embedding the tissues in paraffin. Thereafter, with the help of a microtome, tissue sections of 4-5 µm thickness were prepared and mounted on glass slides. The sections were then subjected to de-paraffinization and rehydration with graded lower ethanol concentrations to distilled water. Staining of sections was executed by submerging them in hematoxylin solution for labelling and visualizing nuclei and subsequent counterstaining with eosin was performed to visualize cellular components and extracellular structures using a light microscope. Histological slides were prepared and the evaluation was performed by a blinded assessor to ensure unbiased analysis of tissue morphology.

Investigation of inflammatory markers

Transcription factor and cytokine gene expression analysis via RT-qPCR: Following the manufacturer's instructions, the cardiac tissue was treated with TRI Reagent® RT (Cat. No: RT 111, Molecular Research Centre, Inc., Cincinnati, OH, USA) to extract RNA from cardiac tissue samples. The quality of isolated RNA was assessed by 260/280 and 260/230 ratios, along with RNA purity and concentration using NanoDrop™ 2000 (USA). The cDNA was synthesized using a SuperScript™ II Reverse Transcriptase (Invitrogen, Thermo Fisher Scientific, USA). Transcript levels were measured using the Eco™ Real-Time PCR System (Illumina, Inc., USA) and SYBR green PCR master mix (Applied Biosystems, Foster City, CA, USA) was employed to amplify the reaction products. GAPDH (Glyceraldehyde-3-phosphate dehydrogenase) was used as a housekeeping gene to normalize the expression of the target genes and the ΔΔCq method was applied to measure fold change of gene expression (Kanno & Hara, 2021). The primers for the target genes (TNF-α, IL-6 and NF-κB p65) were designed using NCBI Primer-BLAST as listed in table 1.

Statistical analysis

Values were presented as mean ± standard error of mean (SEM). Data was normalized for assessing the normal distribution of data using the Shapiro-Wilk test and all variables satisfied the normality criterion. One-way Analysis of variance (ANOVA) was used to compare

groups and Levene's test was implemented to determine the uniformity of variances. Based on the outcomes of Levene's test, post hoc Tukey's test was applied. A p-value < 0.05 was deemed statistically significant. Statistical assessments were undertaken using SPSS version 22.0 (IBM Corp., Armonk, NY, USA).

RESULTS

LA protected against DOX-induced loss of body and heart weight

The animals in the DOX group experienced substantial body weight loss (-12.6 g, $p < 0.001$), highlighting the well-known catabolic effects of DOX compared to control and LA groups, which instead gained weight by 2.3 g and 2.8 g, respectively. However, co-treatment with LA mitigated this body weight loss by (-7.3 g, $p < 0.001$) compared to DOX. Furthermore, a significant reduction was observed in the DOX group compared to the control, LA and LA + DOX groups in absolute heart weight. Analysis of relative heart weight demonstrated that these effects occurred regardless of variations in body weight since the DOX group also exhibited a notable reduction (0.27 ± 0.01) in relative heart weight percentage in comparison to control (0.41 ± 0.04, $P < 0.05$) and LA (0.46 ± 0.03, $P < 0.01$) groups, which was partially reversed by LA co-treatment (0.38 ± 0.01, $p < 0.05$) as shown in table 2.

LA ameliorated DOX-induced systemic toxicity

DOX administration induced marked hematological dysregulation, evidenced by a drop ($p<0.001$) in Hb (9.20 ± 0.22), RBC count (2.17 ± 0.08) and a reduction in hematocrit (27.68 ± 0.12) compared to control (17.20 ± 0.47, 6.77 ± 0.10 and 51.60 ± 0.48, respectively), demonstrating hematopoietic suppression. Moreover, WBC (1.00 ± 0.06), neutrophil (0.58 ± 0.06) and lymphocyte count (0.40 ± 0.06) declined ($p < 0.001$) in comparison to control values (7.33 ± 0.25, 3.65 ± 0.08 and 3.42 ± 0.11, respectively), suggesting an aberrant immune profile. Platelet count (117.17 ± 2.82) was markedly abated ($p < 0.001$) when compared with the control group (296.83 ± 3.84), signifying an Inhibition of hematopoietic activity and a likelihood of coagulation impairment.

Strikingly, LA + DOX group effectively restored **(**$p < 0.001$**)** these hematological anomalies, recovering Hb (13.40 ± 0.50), RBC (3.75 ± 0.08) and hematocrit level (40.17 ± 0.11) while reinstating WBC (3.68 ± 0.13), neutrophil (2.10 ± 0.11), lymphocyte (1.45 ± 0.08) and platelet count (219.17 ± 3.08) compared to the DOX group as shown in fig. 3.

LA ameliorated DOX-induced alterations in lipid and cardiac markers in serum

DOX elicited considerable lipid abnormalities ($p < 0.001$), with a surge in TC (196.33 ± 3.52), TG (143.33 ± 2.24) and LDL (138.33 ± 2.17) levels, whereas HDL (28.16 ± 0.60) levels deteriorated compared to control (137.66 ± 6.37, 105.83 ± 5.48, 75 ± 6.07 and 34.33 ± 1.33, respectively). These changes reflect an atherogenic lipid shift amplifying cardiovascular threat as shown in fig. 4. However, LA + DOX co-administration significantly improved ($p < 0.01$) the levels of HDL (33.5 ± 0.42) and reduced ($p < 0.001$) TC (139.50 ± 1.47), TG (103.83 ± 1.90) and LDL (96 ± 1.18) values compared to the DOX group, providing evidence of LA's lipid modulating response.

Simultaneously, the cardiac damage was confirmed by elevated levels ($p < 0.001$) of CK-MB (21.66 ± 0.88 vs. 13.5 ± 0.76), cTnI (0.65 ± 0.03 vs. 0.058 ± 0.01) and LDH (402.5 ± 4.25 vs. 251.33 ± 10.10) in the DOX group in comparison to the control group, confirming overt myocardial damage**.** Co-treatment group (LA + DOX) exhibited significant reduction ($p < 0.001$) in levels of cTnI (0.33 ± 0.02), LDH (285.66 ± 2.96) and CK-MB ($P < 0.01$,15.16 ± 0.48), compared to the DOX group, suggesting the LA's cardioprotective effect and stabilization of cardiac membrane integrity.

LA reinforces antioxidant defence and mitigates oxidative stress

In fig. 5, A demonstrates that compared to the control (0.0535 ± 0.0006) and LA groups (0.0465 ± 0.0003), the DOX group (0.1447 ± 0.0026) significantly elevated ($p < 0.001$) the levels of MDA, signifying the unchecked oxidative stress. Concomitant depletion ($p < 0.001$) of CAT (19.52 ± 0.35) and SOD (22 ± 1.86) in the DOX group is presented in (B and C), respectively, compared to the control (CAT = 45.90 ± 0.64 and SOD = 38 ± 1.53) and LA groups (CAT = 52.79±0.64 and SOD = 40 ± 1.15), which further corroborated the exhaustion of endogenous antioxidant defenses. Alternatively, LA co-treatment significantly inhibited MDA concentration (0.0864 ± 0.0002, $p < 0.001$), which alludes to reduced lipid peroxidation in cardiac tissue and restored the activity of CAT (32.12 ± 0.38, $p < 0.001$) and SOD (33 ± 1.53, $p < 0.05$) compared to the DOX group, illustrating its antioxidant activity.

LA alleviated DOX-induced histopathological changes in rat cardiac tissue

The histological examination of cardiac tissue of rats from different treatment groups revealed an array of variations from the normal architecture of cardiomyocytes (control group) and partial structural damage with restoration (LA + DOX treated group) to significant injury (DOX group) in fig. 6. The control and LA groups demonstrated no visible evidence of cellular infiltration and degeneration. The structure of cardiac fibers appeared normally aligned and well-organized, with centrally located nuclei in the control and LA groups showing comparable effects (A and B). Pathological changes were observed in cardiac cells in the DOX group, disrupting the normal alignment of cardiac fibres and scattered nuclei. Myofibrillar degeneration was also observed in some cardiac cells due to the appearance of separated and wavy cardiomyocytes.

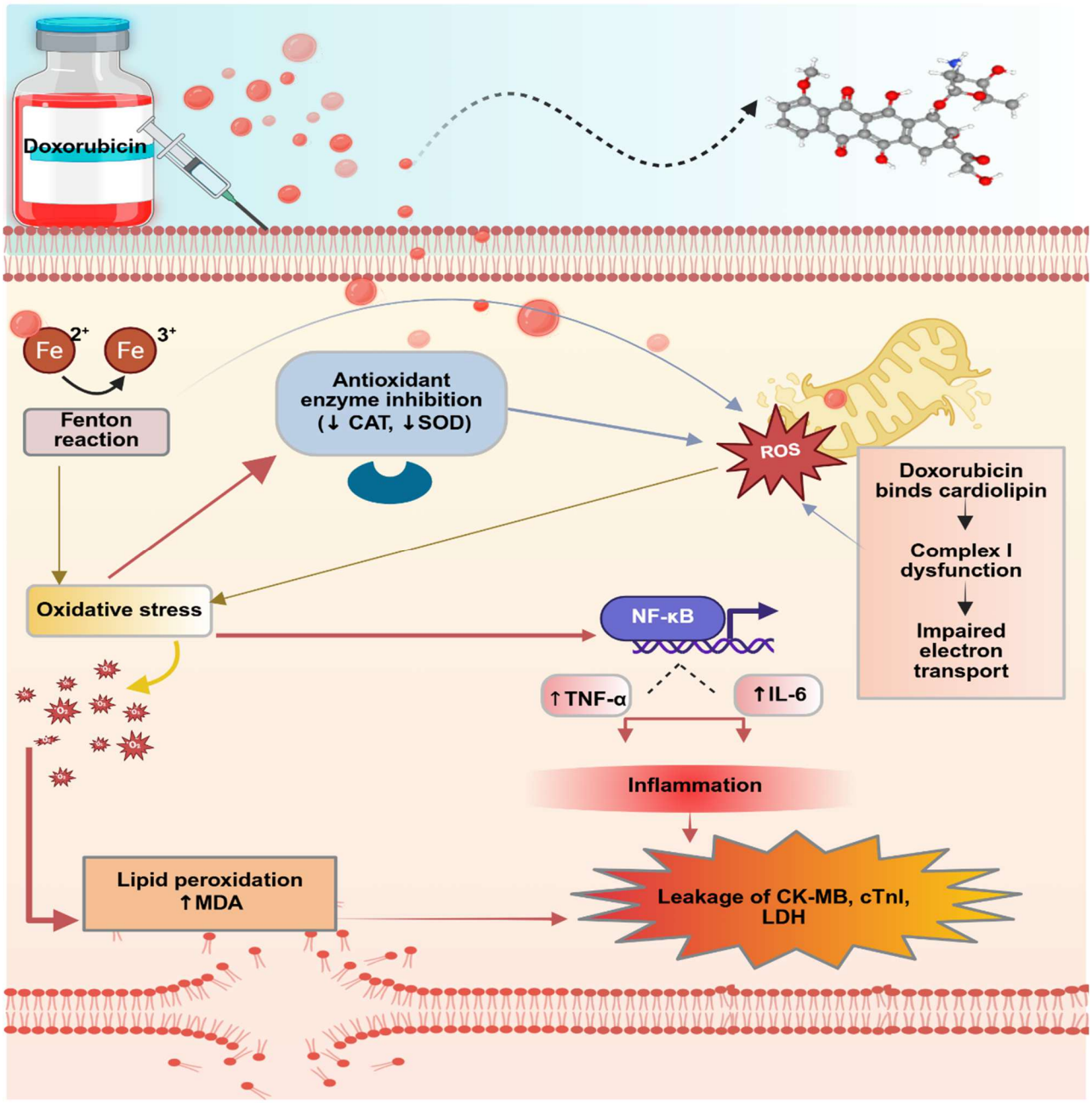

Fig. 1: Schematic representation of the proposed mechanism of DOX-induced oxidative stress. The illustration highlights the iron and mitochondrial-mediated oxidative stress in cardiomyocytes by DOX. In mitochondrial redox cycling, DOX binds cardiolipin in the inner mitochondrial membrane, which disrupts the function of complex I and inhibits ETC. This results in the generation of ROS and, in turn, triggers oxidative stress. In parallel, iron-mediated oxidative stress increases the oxidative burden by generating hydroxyl radical (OH•), created through the Fenton reaction [(The ferrous ion (Fe^{2+}) donates an electron to hydrogen peroxide (H_2O_2), leading to the formation of a ferric ion (Fe^{3+})]. Oxidative stress triggers lipid peroxidation (increased MDA levels) and inhibits the activity of endogenous antioxidant enzyme systems, including CAT and SOD. Oxidative stress also promotes the activation of NF-κB, which enhances the transcription of TNF-α and IL-6. The pro-inflammatory cytokines result in myocardial inflammation. Together with lipid peroxidation and activation of the inflammatory cascade, cardiomyocyte damage occurs, which is reflected by the release of CK-MB, cTnI, and LDH in serum. (DOX: doxorubicin, ETC: electron chain transport, ROS: reactive oxygen species, MDA: malondialdehyde, CAT: catalase, SOD: superoxide dismutase, NF-κB: nuclear factor kappa-light-chain-enhancer of activated B cells, TNF-α: tumor necrosis factor-alpha, IL-6: interleukin-6, CK-MB: creatine kinase – MB, cTnI: cardiac troponin I, LDH: lactate dehydrogenase). Created with BioRender. Aziz, S. (2025) https://BioRender.com/fne3ohy.

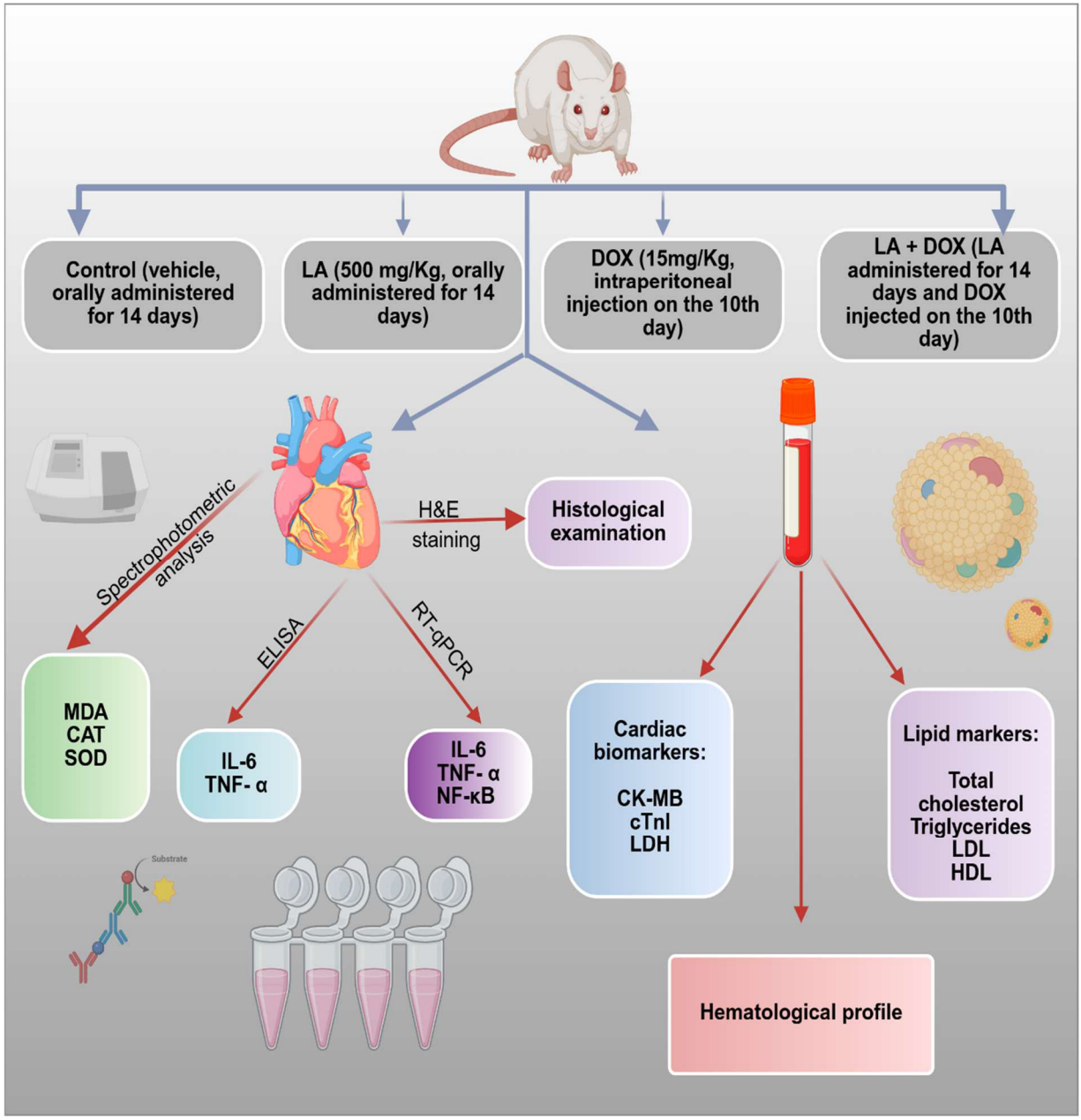

Fig. 2: Experimental workflow for evaluating the cardioprotective role of LA in DOX-mediated cardiotoxicity in rats. Created with BioRender. Aziz, S. (2025) https://BioRender.com/nyrpooi.

Tissue injury can be confirmed by infiltration of inflammatory cells, evidenced by a cluster of dark-stained nuclei. Cytoplasmic vacuolation and loss of nuclei in cardiac fibers around the infiltration indicate cellular damage and myocyte necrosis (C). Co-administration of LA + DOX showed mild damage and fairly preserved cardiomyocytes with visible and elongated nuclei in most areas. Mild-to-moderate infiltration was seen with dispersed inflammatory cells and overall restoration of cardiac structure compared to the DOX group (D), suggesting the cardioprotective effect of LA in DOX-induced cardiotoxicity.

LA suppresses NF-κB-mediated inflammatory pathways

As illustrated in fig. 7, DOX triggered a marked inflammatory activity in rats, demonstrated by significant upregulation of key pro-inflammatory genes. mRNA expressions of NF-κB p65, IL-6 and TNF-α were increased by 2.6-fold, 4-fold and 3-fold ($p<0.001$ vs. LA) (A-C). respectively. This transcriptional surge was paralleled by changes in the protein levels in the DOX group, showing increased ($p < 0.001$) IL-6 (7.4 ± 0.0577) (D) and TNF-α (5.85 ± 0.0058) concentrations (E) in cardiac tissue compared with control (IL-6 = 0.68 ± 0.0058 and TNF-α = 0.208 ± 0.00153) and LA values (IL-6 = 0.56 ± 0.0058 and TNF-α = 0.073 ±0.000577).

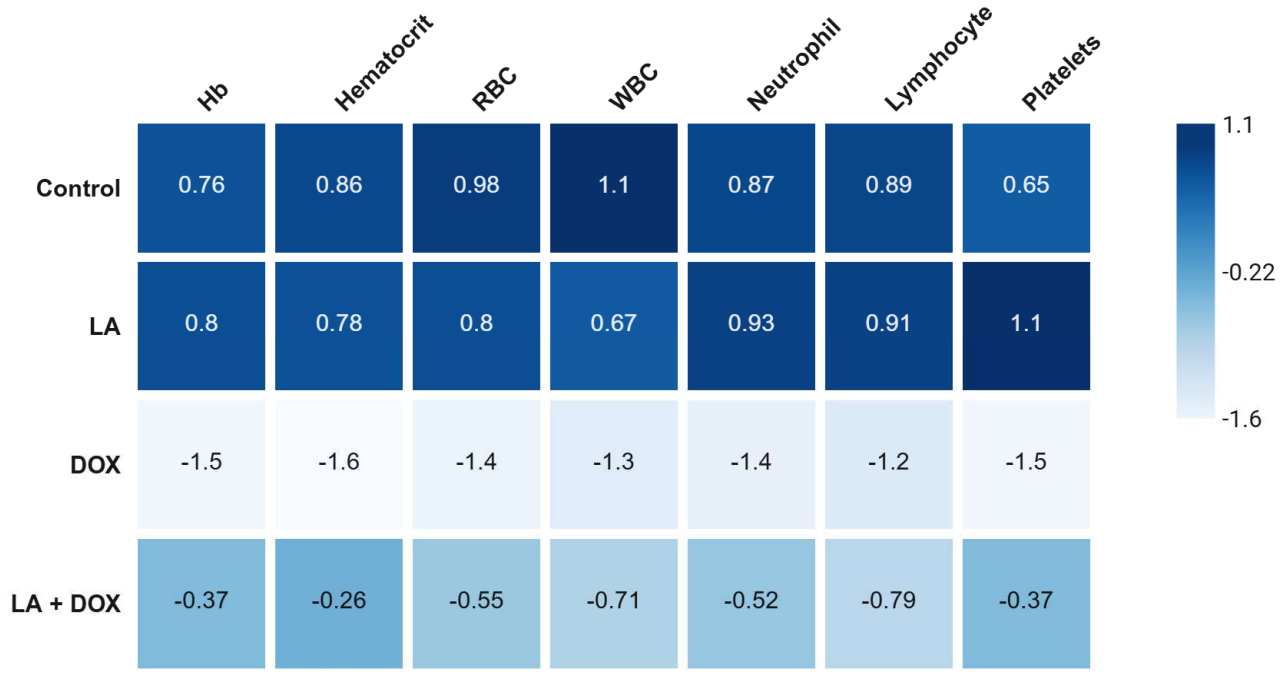

Fig. 3: LA ameliorated DOX-induced alterations in the hematological profile. Rats were administered 15 mg/kg DOX with or without LA (500 mg/kg for 14 days). Heatmap displaying the relative levels of hematological parameters including Hb (g/dL), hematocrit (%), RBC (10^{12}/L), WBC (10^9/L), neutrophil (10^9/L), lymphocyte (10^9/L) and platelets (10^9/L) (n = 6); their mean values were normalized by z-scoring. The color gradient ranges from dark blue, indicating the highest z-scores, to white, indicating the lowest z-scores, with a light blue color representing values near the group mean. Each column represents a hematological parameter, and each row corresponds to an individual group.

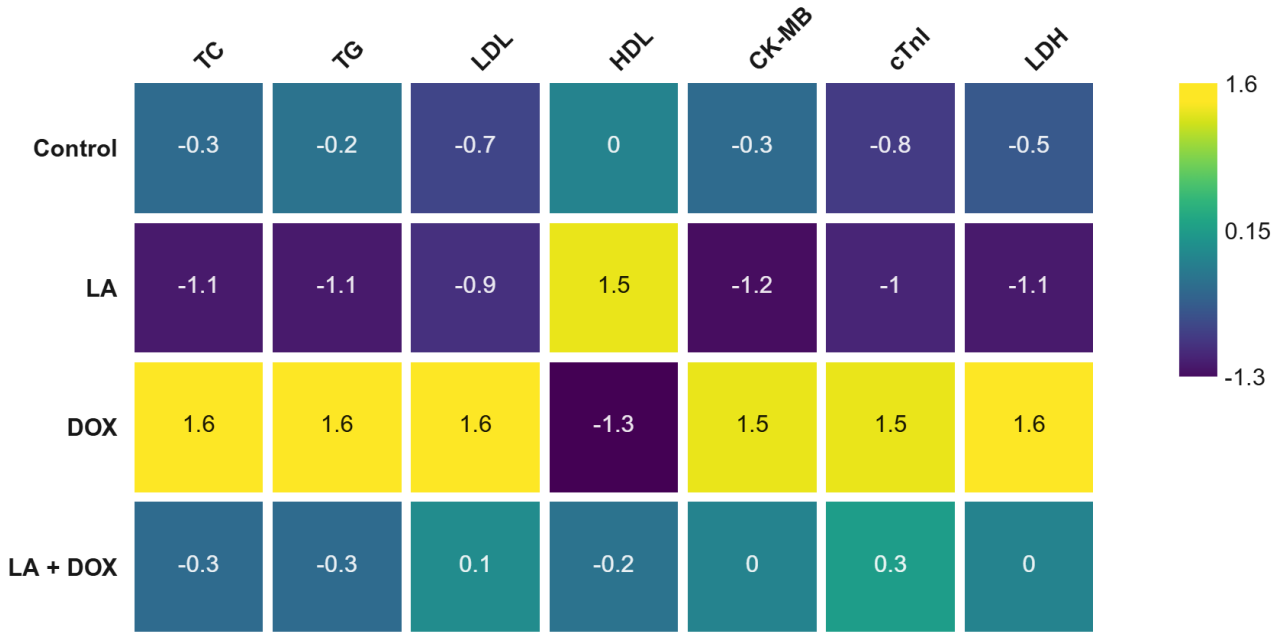

Fig. 4: LA ameliorated DOX-induced alterations in lipid and cardiac markers in serum. Rats were administered 15 mg/kg DOX with or without LA (500 mg/ kg for 14 days). Heatmap displaying the relative serum levels of lipid markers, including TC (mg/dL), TG (mg/dL), LDL (mg/dL), and HDL (mg/dL), and cardiac biomarkers, including CK-MB (IU/L), cTnI (ng/mL) and LDH (U/L) (n = 6); their mean values were normalized by z-scoring. The color gradient ranges from yellow, representing the highest z-scores, to purple, the lowest z-scores, with a blue color representing values near the group mean. Each column represents a lipid or cardiac marker, and each row corresponds to an individual group.

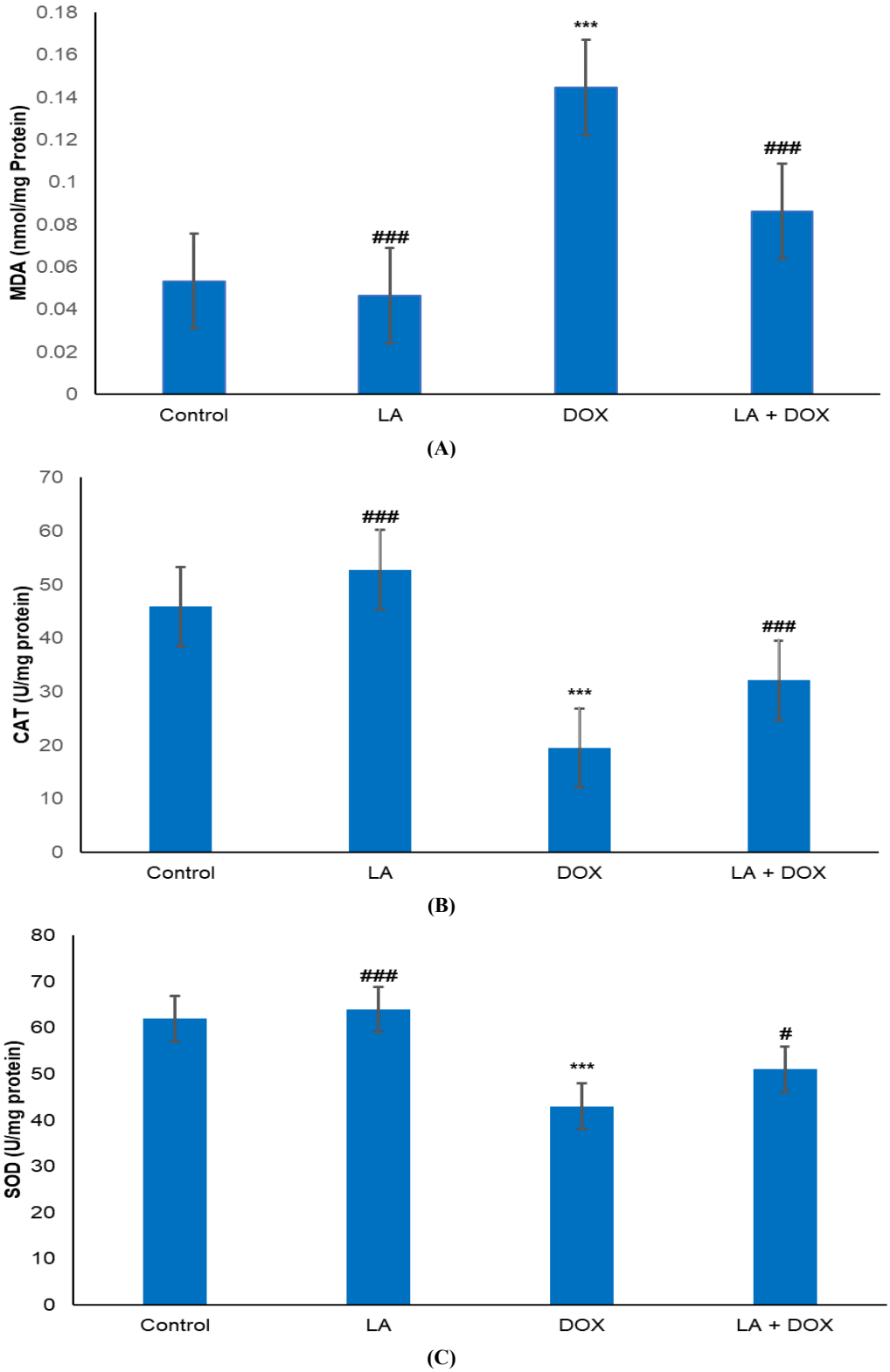

Fig. 5: LA attenuated DOX-mediated myocardial lipid peroxidation and oxidative stress. Rats were administered 15 mg/kg DOX with or without LA (500 mg/kg, for 14 days), and (A) MDA (nmol/mg protein) concentration was assessed by TBARS assay. (B) CAT (U/mg protein) and (C) SOD (U/mg protein) levels were evaluated in cardiac tissue using microassay commercial kits (n = 6). One-way ANOVA was applied for statistical analysis, followed by post hoc Tukey's test using SPSS version 22.0. $^{***}P < 0.001$ when compared with control. $^{###}P < 0.001$, $^{#}P < 0.05$ when compared with DOX.

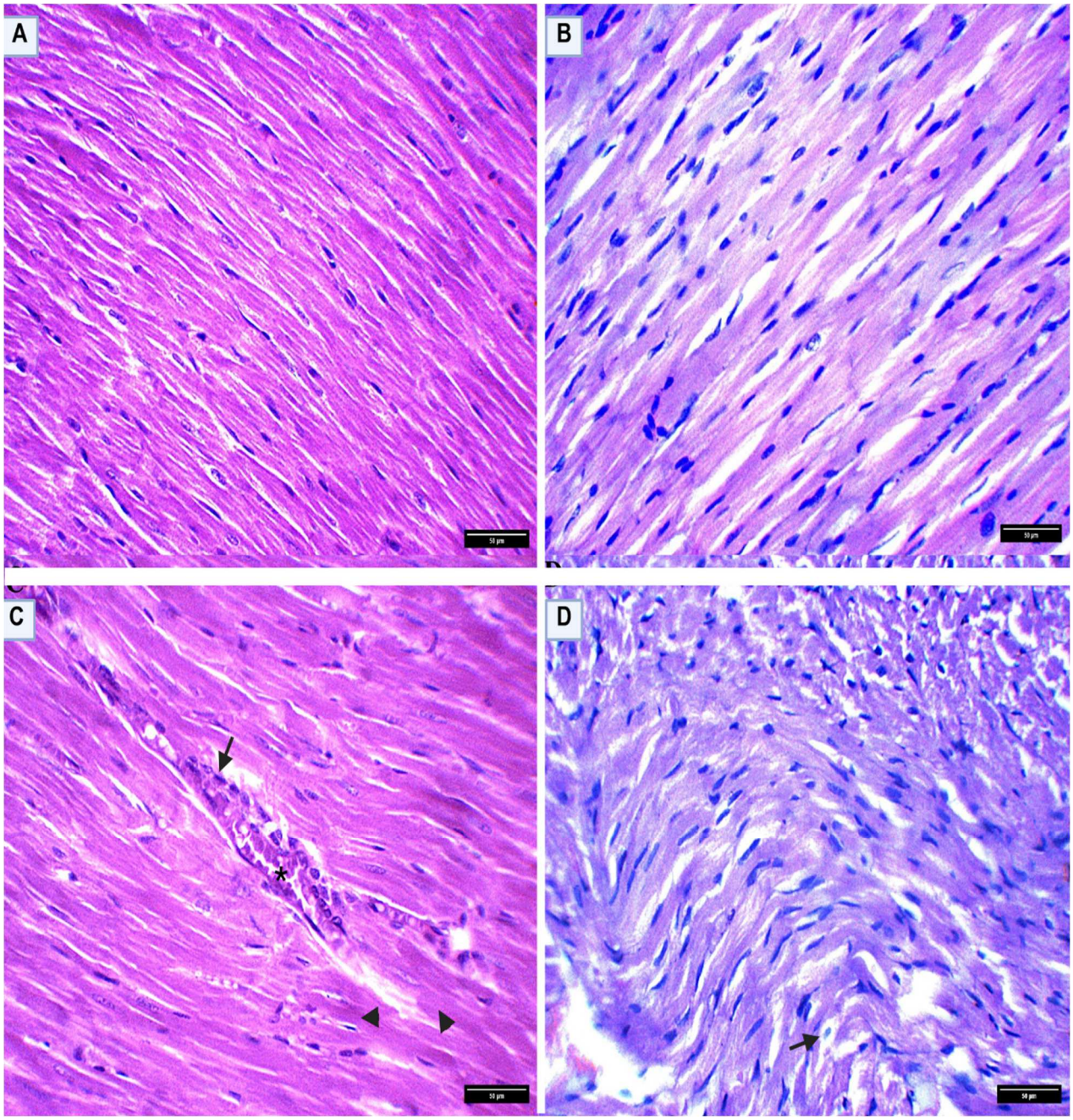

Fig. 6: LA alleviated DOX-induced histopathological changes in rat cardiac tissue. Rats were administered 15 mg/kg DOX with or without LA (500 mg/kg, for 14 days), and cardiac sections were stained with hematoxylin-eosin staining and observed under 40x magnification of the light microscope. (A) exhibits a cardiac section from the control group with normal morphology. (B) shows a cardiac section from the LA group with normal shape and size of cardiomyocytes. (C) presents a cardiac section from the DOX group with the irregular shape of myofibrils (arrowhead), clustering of nuclei (asterisk), and leukocyte infiltration (arrow) showing signs of inflammation. (D) shows a cardiac section of the combined treatment group of LA + DOX with partially protected myocytes and scattered inflammatory cells (arrow), demonstrating the cardioprotective effect of LA.

LA co-treatment attenuated ($p < 0.001$) this inflammatory cascade, downregulating the gene expressions of NF-κB p65 (1.8-fold), IL-6 (2.5-fold) and TNF-α (1.9-fold). Consequently, LA significantly lowered ($p < 0.001$) the protein levels of IL-6 (3.54 ± 0.0058) and TNF-α (2.167 ± 0.0006) in cardiac tissue compared to the DOX group, validating its strong anti-inflammatory effects at both transcriptional and translational levels.

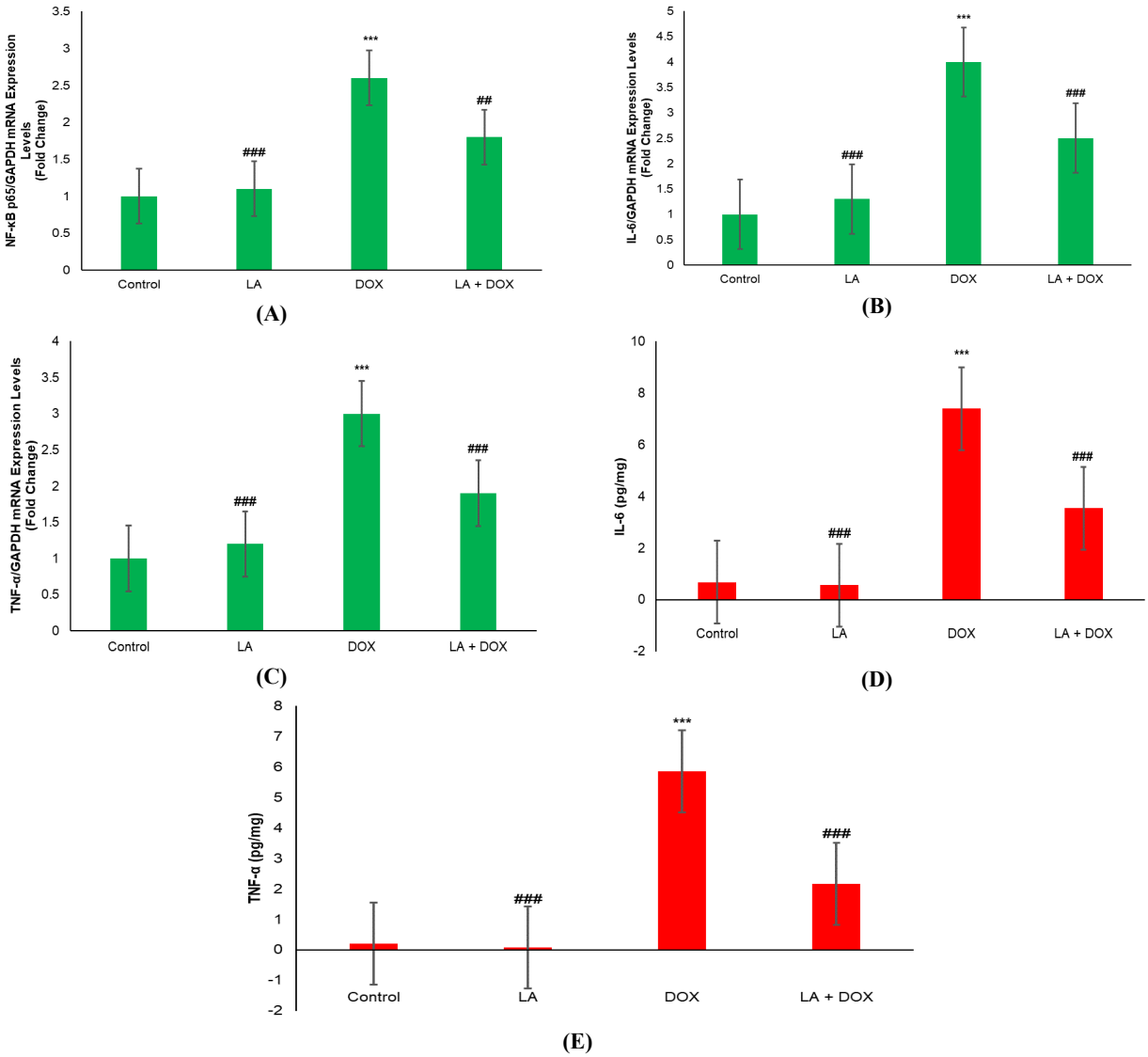

Fig. 7: LA mitigated DOX-induced inflammation in rats. Rats were administered 15 mg/kg DOX with or without LA (500 mg/kg, 14 days), and mRNA expression levels (fold change) of transcription factor, (A) NF-κB and inflammatory cytokines; (B) IL-6 and (C) TNF-α were measured by RT-qPCR. Protein levels of (D) IL-6 and (E) TNF-α were assessed in cardiac tissue using commercial ELISA kits. One-way ANOVA was applied for statistical analysis, followed by post hoc Tukey's test using SPSS version 22.0. ***P <0.001 when compared with control. $^{###}$P < 0.001, $^{##}$P < 0.01 when compared with DOX.

Moreover, the result summary of the comparison in hematological parameters, lipid profile, cardiac markers, oxidative stress markers and inflammatory cytokines among different experimental groups is listed in table 3.

DISCUSSION

Our study showed that LA, a naturally occurring medium-chain saturated fatty acid, efficiently disrupted the destructive progression of cardiotoxicity caused by DOX by preserving the myocardial architecture and its function. The DOX-mediated adverse effects were initially demonstrated by a considerable reduction in both body and heart weights, likely due to suppressed appetite and disturbances in basal metabolic activities, which are often correlated with the loss of myocardial tissue mass as a result of necrosis and atrophy in cardiomyocytes (Maghraby *et al*., 2025). Multiple catabolic pathways are triggered, including proteolytic signaling, ubiquitin-proteasome system and autophagy as a result of dox-mediated oxidative stress and mitochondrial dysfunction, which promote skeletal muscle atrophy and weight loss (Hiensch *et al*., 2020). LA treatment preserved the body and heart weight changes induced by DOX administration, which is likely due to its ability to limit oxidative stress and reverse mitochondrial damage. Our findings suggest that LA reduced oxidative stress in cardiac tissue, as indicated

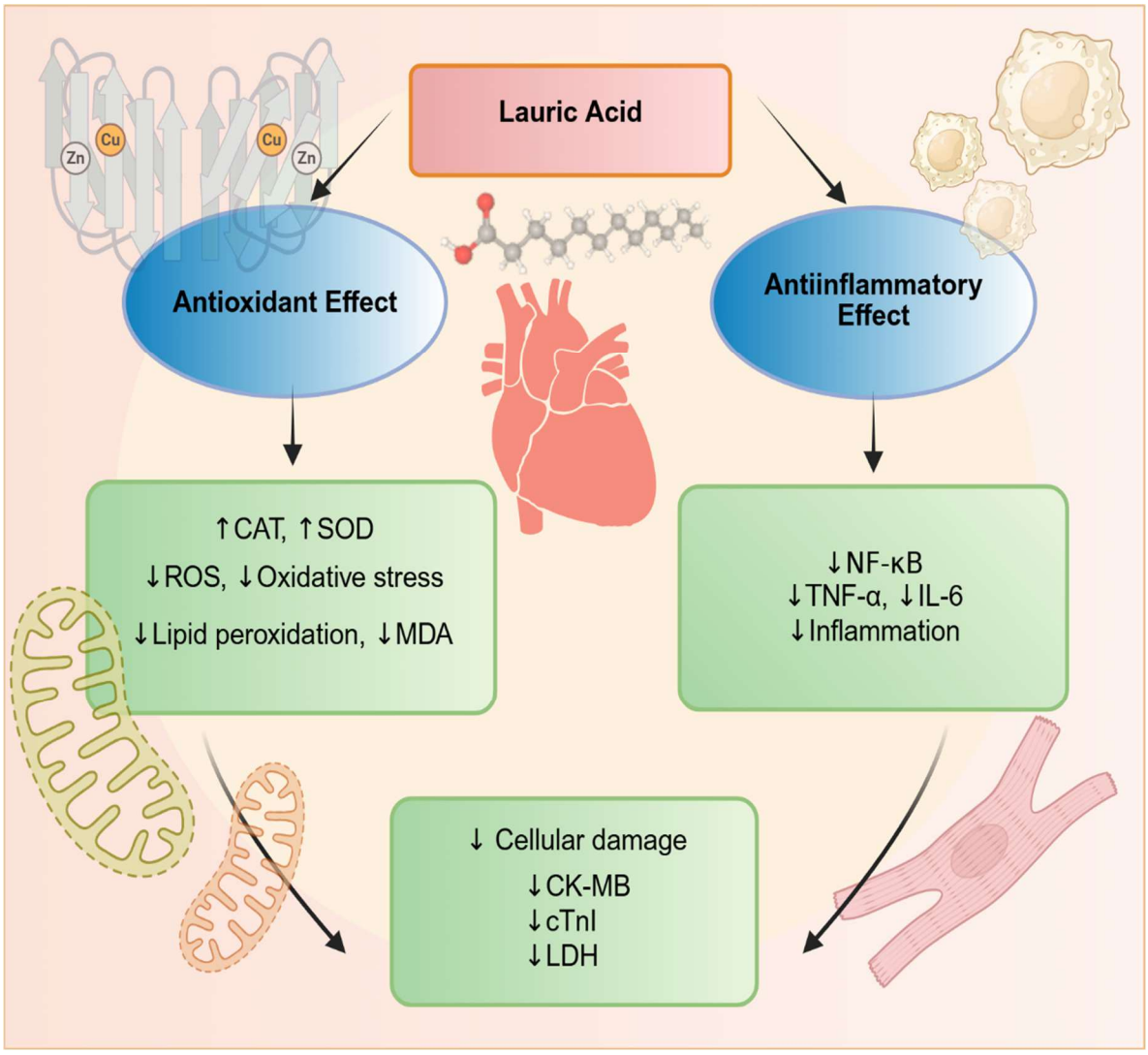

Fig. 8: Suggested cardioprotective mechanism of LA in DOX-induced oxidative and inflammatory injury in cardiac cells. Created with BioRender. Aziz, S. (2025) https://BioRender.com/qah96we

by decreased MDA and increased antioxidant enzyme levels (SOD and CAT).

Interestingly, a recent study in colorectal cancer cells demonstrated that LA reprogrammed energy metabolism by shifting glycolytic cells to oxidative phosphorylation (OXPHOS), a process dependent on mitochondrial activation (Fujiwara-Tani *et al*., 2025). Although the metabolic context and cellular outcomes differ, this provides indirect evidence that LA may restore or enhance mitochondrial activity under stress conditions, which could partially explain its cardioprotective effect against DOX-induced mitochondrial dysfunction. This aligns well with previously reported studies on the improvement in body weight in experimental animals with compounds possessing antioxidant potential (do Nascimento Filho *et al*., 2025; Liao *et al*., 2023).

Exposure to DOX imposed a marked oxidative burden on the myocardium, as demonstrated by increased levels of MDA, a key marker of lipid peroxidation. The unregulated accumulation of ROS not only impairs cardiac cell membranes and disrupts systemic lipid homeostasis, as evidenced by the increase in TC, TG and LDL, but also a concurrent decline in HDL (Goje *et al*., 2025). This dyslipidemic state, fueled by oxidative stress, exacerbated endothelial dysfunction and accelerated atherogenic pathways (Ifeanacho *et al*., 2021). However, LA treatment rapidly mitigated these changes; its antioxidative action may have suppressed ROS production, subsequently diminishing lipid peroxidation and restoring serum lipid markers. This combined modulation suggests that LA's capacity to shield lipid-metabolizing enzymes from oxidative insults, correcting lipid dysregulation at a critical juncture. LA improved the lipid profile, possibly due to its antioxidant properties, as reported by previous research studies (Anuar *et al*., 2023b; Namachivayam & Gopalakrishnan, 2023).

Table 1: RT-qPCR primers used in the study.

Gene	GenBank accession number	Primer sequence (5'-3')
TNF-α	NM_012675.3	F: CCAGACCCTCACACTCAGTAAG
		R: CTTAGGTTTCCCAGCAAGCA
IL-6	NM_012589.2	F: CTCACACTCCTCTCACAGTCT
		R: CGAAAGTCAACTCCATCTGCC
NF-κB p65 (RELA)	NM_199267.2	F: CCATTAGCCAGCGCATCCAG
		R: AGTGTTGGGGGCACGGTTA
GAPDH	NM_017008.4	F: GTTACCAGGGCTGCCTTCTC
		R: TGAGGTCAATGAAGGGGTCG

Measurement of cytokine levels using ELISA: Protein levels of TNF-α and IL-6 in cardiac tissue were analyzed using commercial ELISA kits following the manufacturer's instructions.

Table 2: LA reversed the DOX-induced reduction in body weight and heart weight in rats

Groups	Initial body weight (g)	Final body weight (g)	Body weight change (g)	Absolute heart weight (g)	Relative heart weight (%)
Control	240.5 ± 1.40	242.8 ± 1.40	2.3 ± 0.52	1.01 ± 0.10	0.41 ± 0.04
LA	223.7 ± 1.50	226.5 ± 1.30	$2.8 \pm 0.48^{\#\#\#}$	$1.05 \pm 0.0^{\#\#}$	$0.46 \pm 0.03^{\#\#}$
DOX	244.8 ± 2.10	225.8 ± 1.60	$-12.6 \pm 0.45^{***}$	$0.63 \pm 0.01^{**}$	$0.27 \pm 0.01^{*}$
LA + DOX	243.8 ± 2.10	236.5 ± 1.90	$-7.3 \pm 1.3^{\#\#\#}$	0.91 ± 0.02	$0.38 \pm 0.01^{\#}$

Rats were administered 15 mg/kg DOX with or without LA (500 mg/kg, 14 days) (n = 6). The data are reported as mean ± SEM. For statistical analysis, One-way ANOVA was applied, followed by post hoc Tukey's test using SPSS version 22.0. ***P <0.001, **P <0.01, *P <0.05 when compared with control. $^{\#\#\#}$P < 0.001, $^{\#\#}$P < 0.01, $^{\#}$P < 0.05 when compared with DOX.

Table 3: Summary of comparison in hematological parameters, lipid profile, cardiac markers, oxidative stress markers, and inflammatory cytokines among different experimental groups. No significant changes were observed in the LA-only group compared to the control for all parameters assessed

Parameters	DOX vs. control	LA + DOX vs. DOX
Hemoglobin	↓ 46.5 %	↑ 45.7%
Hematocrit	↓ 46.4%	↑ 45.2%
RBC	↓ 67.9%	↑ 72.8%
WBC	↓ 86.4%	↑ 254.0%
Neutrophils	↓ 84.1%	↑ 262.1%
Lymphocytes	↓ 88.3%	↑ 262.5%
Platelets	↓ 60.5%	↑ 87.1%
Total cholesterol	↑ 1.3%	↓ 25.6%
Triglycerides	↑ 26.5%	↓ 28.3%
LDL	↑ 28.0%	↓ 27.9%
HDL	↓ 18.0%	↑ 19.0%
CK-MB	↑ 60.4%	↓ 30.0%
cTnI	↑ 983.3%	↓ 49.2%
LDH	↑ 60.1%	↓ 29.0%
MDA	↑ 170.5%	↓ 40.3%
CAT	↓ 30.0%	↑ 25.1%
SOD	↓ 42.1%	↑ 50.0%
IL-6 (mRNA Expression)	↑ 200.0%	↓ 50.0%
TNF-α (mRNA Expression)	↑ 220.0%	↓ 40.6%
NF-κB p65 (mRNA Expression)	↑ 250.0%	↓ 40.0%
IL-6 (Protein Levels)	↑ 988.2%	↓ 52.2%
TNF-α (Protein Levels)	↑ 2712.0%	↓ 63.0%

Percentages in the "DOX vs. control" column show the percentage increase (↑) or decrease (↓) in the dox group compared to the control group. Percentages in the "LA + DOX vs DOX" column represent the extent of improvement observed in the LA + DOX group compared to the DOX group. ↑ = increase; ↓ = decrease

Other agents have been explored for their potential to protect against DOX-induced cardiotoxicity. For example, compounds like curcumin**,** coenzyme Q10 and melatonin have demonstrated protective effects through mechanisms such as reducing oxidative stress, improving lipid profiles and alleviating inflammation (Botelho *et al*., 2020; Ibrahim Fouad & Ahmed, 2022; Zhang *et al*., 2023).

The structural vulnerability caused by ROS and dyslipidemia elicited the cardiomyocyte injury, as reflected by the escape of cardiac biomarkers, CK-MB, cTnI and LDH into the systemic circulation, which typically mirrors the underlying membrane damage (Pan *et al*., 2022). The intervention of LA was demonstrated to be pivotal here, as it alleviated oxidative stress and protected the membrane structure, significantly reducing the efflux of these myocardial injury markers. Consequently, LA maintained myocardial viability against the cardiotoxic effects of DOX. A study documenting the cardioprotective role of extra-virgin coconut oil, rich in LA, found that it lowered the levels of cardiac markers, particularly CK-MB and LDH, in experimental animals (NADIAH *et al*., 2023).

Simultaneously, the oxidative stress caused by DOX overburdened the endogenous antioxidant defenses, reducing critical enzymes such as SOD and CAT. The main target of SOD is superoxide anion (O_2-) to convert it into hydrogen peroxide (H_2O_2) and oxygen, diminishing the initial ROS load that is responsible for cellular damage. H_2O_2 is subsequently catalyzed by CAT, leading to its conversion into oxygen and water, which helps mitigate the accumulation of H_2O_2, cessation of which can contribute to the initiation of Fenton's reaction and formation of highly reactive hydroxyl radicals (OH•) (Ighodaro & Akinloye, 2018) This deterioration further escalated ROS accumulation, exacerbating cardiac damage in a recursive pattern. Yet, LA intervention restored the antioxidant enzymes, increasing the levels of SOD and CAT and thereby strengthening the myocardium against oxidative burden. The outcomes are consistent with a recent study performed (Sedik *et al*., 2024).

In addition to oxidative stress and lipid-mediated damage, DOX spurred a pronounced inflammatory response, as reflected by the augmented expression of inflammatory cytokines (TNF-α and IL-6) at both the transcript and protein levels and transcription factor NF-κB p65. These cytokines are not only associated with activating the NF-κB pathway involved in transcriptional modulation of TNF-α and IL-6 (Pecoraro *et al*., 2016). Still, they are also known to initiate apoptotic signaling and fibrotic remodeling [38], which further impairs cardiac function. Histopathological examination supported this, revealing myofibrillar misalignment, cytoplasmic vacuolization and inflammatory cell infiltration in DOX-treated myocardium (Shaker *et al*., 2018). Intriguingly, gene expression and protein levels of the inflammatory cytokines and NF-κB in cardiac tissue were downregulated with LA treatment, reflecting the down regulation of NF-κB pathway activation. This anti-inflammatory action of LA was corroborated with the histological preservation observed, wherein LA-treated cardiac tissue maintained the structural integrity of cardiac cells and minimal inflammatory damage. Our findings are in harmony with existing reported studies about exploring the anti-inflammatory potential of LA (Huang *et al*., 2014; Khan *et al*., 2021). Besides the cardiotoxic effects, DOX-induced adverse systemic effects manifest as compromised hematological indices, including decreased hemoglobin, RBC count, hematocrit and low WBC and platelet counts (Sergazy *et al*., 2020). The altered hematological parameters are mainly due to the myelosuppressive effects of DOX (Chen *et al*., 2017). Furthermore, thrombocytopenia elevates the risk of hemorrhage, thereby worsening the overall morbidity linked to DOX toxicity (Ma *et al*., 2022). Additional support for LA's systemic protective effect is demonstrated by normalizing hematological parameters, likely by alleviating inflammation, reducing oxidative damage in the bone marrow and facilitating erythropoiesis.

These findings emphasized the complex interconnection of oxidative stress, dyslipidemia, cardiac tissue injury and inflammation in the pathogenesis of DOX-mediated cardiotoxicity. By strategically focusing on each pathological state as it developed, LA exhibited a wide-ranging cardioprotective effect, highlighting its potential therapeutic value in mitigating chemotherapy-induced damage to cardiac tissue. Fig. 8 illustrates the cardioprotective role of LA in DOX-induced oxidative and inflammatory injury. While our study highlights the cardioprotective effects of LA through modulation of oxidative stress and inflammation, it is important to acknowledge potential upstream and downstream mediators not directly assessed in this model. Upstream, the transcription factor Nrf2, a key regulator of antioxidant gene expression, may contribute to the increased SOD and CAT levels observed following LA treatment. Similarly, inhibition of Toll-like receptor (TLR) signaling could underlie the down regulation of NF-κB and inflammatory cytokines. Downstream, caspase activation, apoptotic signaling, or fibrotic remodeling could be involved in the myocardial damage seen in DOX-treated rats and may be mitigated by LA. Although these mediators were not directly measured, future studies are warranted to explore these mechanistic links and validate the broader signaling pathways through which LA exerts cardioprotection.

CONCLUSION

These results suggest that LA alleviates DOX-induced cardiotoxicity in rats and exhibits its potential to serve as an adjuvant to prevent chemotherapy-induced cardiac damage. Before integrating the findings of this preclinical study into a clinical setting, future studies should focus on comprehensive preclinical evaluation and dose optimization to support translational relevance. The effects

of LA could further be explored as a synergistic agent when administered in combination with other antioxidants for enhanced cardioprotection.

Acknowledgement
The authors would like to express their gratitude to all individuals who contributed to this work directly or indirectly.

Author's contributions
Samreen Aziz conceived and designed the study, performed the experiments, analyzed the data, and prepared the manuscript draft. Humera Khatoon supervised the project and provided overall guidance. Aisha Aziz assisted in experimentation. Muhammad Imran performed statistical analysis. Azfar Athar Ishaqui contributed in proofreading and final review of the manuscript. All authors read and approved the final version of the manuscript.

Funding
This research did not receive any specific grant from funding agencies in the public, commercial, or not-for-profit sectors.

Data availability statement
All data generated or analyzed during this study are included in this published article [and its supplementary information files].

Ethical approval
Animal care and handling were followed by NIH (National Institute of Health) guidelines (8th ed., National Research Council, 2011) and the study was approved by the institutional ethical review board of Jinnah University for Women, Karachi, Pakistan (JUW/IERB/PHARM-ARA-011/2025).

Conflict of interest
The authors declare that they have no conflicts of interest concerning this article.

Supplementary data
https://www.pjps.pk/uploads/2025/12/SUP1766899001.pdf

REFERENCES

Akula ST, Nagaraja A, Ravikanth M, Kumar NGR, Kalyan Y and Divya D (2021). Antifungal efficacy of lauric acid and caprylic acid-Derivatives of virgin coconut oil against Candida albicans. *Biomed. Biotechnol. Res. J.*, **5**(2): 229-234.

Alharbi FK, Alshehri ZS, Alshehri FF, Alhajlah S, Khalifa HA, Dahran N and Ghonimi WA (2023). The role of hesperidin as a cardioprotective strategy against doxorubicin-induced cardiotoxicity: The antioxidant, anti-inflammatory, antiapoptotic and cytoprotective potentials. *Open Vet. J.*, **13**(12): 1718.

Alves NFB, de Queiroz TM, de Almeida Travassos R, Magnani M and de Andrade Braga V (2017). Acute treatment with lauric acid reduces blood pressure and oxidative stress in spontaneously hypertensive rats. *Basic Clin. Pharmacol. Toxicol,*, **120**(4): 348-353.

Angsutararux P, Luanpitpong S and Issaragrisil S (2015). Chemotherapy-induced cardiotoxicity: overview of the roles of oxidative stress. *Oxid. Med. Cell Longev.*, **2015**(1): 795602.

Anuar NS, Shafie SA, Maznan MAF, Zin NSNM, Azmi NAS, Raoof RA, Myrzakozha D and Samsulrizal N (2023a). Lauric acid improves hormonal profiles, antioxidant properties, sperm quality and histomorphometric changes in testis and epididymis of streptozotocin-induced diabetic infertility rats. *Toxicol. Appl. Pharmacol.*, **470**: 116558.

Anuar NS, Shafie SA, Maznan MAF, Zin NSNM, Azmi NAS, Raoof RA, Myrzakozha D and Samsulrizal N (2023b). Lauric acid improves hormonal profiles, antioxidant properties, sperm quality and histomorphometric changes in testis and epididymis of streptozotocin-induced diabetic infertility rats. *Toxicol. Appl. Pharmacol.*, **470**: 116558.

Aryal B and Rao VA (2016). Deficiency in cardiolipin reduces doxorubicin-induced oxidative stress and mitochondrial damage in human B-lymphocytes. *PloS One*, **11**(7): e0158376.

Botelho AFM, Lempek MR, Branco SEM, Nogueira MM, de Almeida ME, Costa AG, Freitas TG, Rocha MCR, Moreira MV and Barreto TO (2020). Coenzyme Q10 cardioprotective effects against doxorubicin-induced cardiotoxicity in Wistar rat. *Cardiovasc. Toxicol.*, **20**: 222-234.

Chen T, Shen HM, Deng ZY, Yang ZZ, Zhao RL, Wang L, Feng ZP, Liu C, Li WH and Liu ZJ (2017). A herbal formula, SYKT, reverses doxorubicin-induced myelosuppression and cardiotoxicity by inhibiting ROS-mediated apoptosis. *Mol. Med. Rep.*, **15**(4): 2057-2066.

Do Nascimento Filho AV, Stoyell-Conti FF, Gauri A, Lima LSS, Bernardes N, Irigoyen MC, Singal P, De Angelis K and da Silva Dias D (2025). Vitamin C protects against doxorubicin induced skeletal muscle atrophy: Role of oxidative stress. *Can. J. Physiol. Pharmacol.*, **103**(6): 0154.

Dubo A, Dawud F, Umar I, Alex E, Baiyekusi S and Farra'u U (2019). Lauric acid alleviates inflammation and structural changes in the lungs of type II diabetic male Wistar rats. *J. Afr. Ass. Physiol. Sci.,* **7**(2): 88-96.

El-Agamy DS, El-Harbi KM, Khoshhal S, Ahmed N, Elkablawy MA, Shaaban AA and Abo-Haded HM (2018). Pristimerin protects against doxorubicin-induced cardiotoxicity and fibrosis through modulation of Nrf2 and MAPK/NF-kB signaling pathways. *Cancer Manag. Res.*, **2019**(11): 47-61.

Fujiwara-Tani R, Luo Y, Ogata R, Fujii K, Sasaki T, Sasaki R, Nishiguchi Y, Mori S, Ohmori H and Kuniyasu H (2025). Energy metabolism and stemness and the role of lauric acid in reversing 5-fluorouracil resistance in colorectal cancer cells. *Int. J. Mol. Sci.*, **26**(2): 664.

Goje ID, Goje GI, Ordodi VL, Ciobotaru VG, Ivan VS, Buzaș R, Tunea O, Bojin F and Lighezan DF (2025). Doxorubicin-induced cardiotoxicity and the emerging role of SGLT2 inhibitors: From glycemic control to cardio-oncology. *Pharmaceuticals (Basel)*, **18**(5): 681.

Hany AAH, Zainab NM, Ali HA and Meena AN (2022). Panax ginseng as antioxidant and anti-inflammatory to reduce the cardiotoxicity of doxorubicin on rat module. *Res. J. Pharm. Technol.*, **15**(10): 4594-4600.

Hiensch AE, Bolam KA, Mijwel S, Jeneson JA, Huitema AD, Kranenburg O, Van der Wall E, Rundqvist H, Wengstrom Y and May AM (2020). Doxorubicin-induced skeletal muscle atrophy: Elucidating the underlying molecular pathways. *Acta Physiol. (Oxf).*, **229**(2): e13400.

Huang WC, Tsai TH, Chuang LT, Li YY, Zouboulis CC and Tsai PJ (2014). Anti-bacterial and anti-inflammatory properties of capric acid against Propionibacterium acnes: A comparative study with lauric acid. *J. Dermatol. Sci.*, **73**(3): 232-240.

Ibrahim Fouad G and Ahmed KA (2022). Curcumin ameliorates doxorubicin-induced cardiotoxicity and hepatotoxicity via suppressing oxidative stress and modulating iNOS, NF-κB and TNF-α in rats. *Cardiovasc. Toxicol.*, **22**(2): 152-166.

Ifeanacho MO, Ikewuchi JC, Ikewuchi CC, Nweke PC, Okere R and Nwate TL (2021). Prevention of doxorubicin-induced dyslipidaemia, plasma oxidative stress and electrolytes imbalance in Wistar rats by aqueous leaf-extracts of *Chromolaena odorata* and *Tridax procumbens*. *Sci. Afr.*, **11**: e00636.

Ighodaro O and Akinloye O (2018). First line defence antioxidants-superoxide dismutase (SOD), catalase (CAT) and glutathione peroxidase (GPX): Their fundamental role in the entire antioxidant defence grid. *ALEX. J. Med.,* **54**(4): 287-293.

Kanno SI and Hara A (2021). The mRNA expression of Il6 and Pdcd1 are predictive and protective factors for doxorubicin-induced cardiotoxicity. *Mol. Med. Rep.*, **23**(2): 113.

Khan HU, Aamir K, Jusuf PR, Sethi G, Sisinthy SP, Ghildyal R and Arya A (2021). Lauric acid ameliorates lipopolysaccharide (LPS)-induced liver inflammation by mediating TLR4/MyD88 pathway in Sprague Dawley (SD) rats. *Life Sci.*, **265**: 118750.

Liao D, Shangguan D, Wu Y, Chen Y, Liu N, Tang J, Yao D and Shi Y (2023). Curcumin protects against doxorubicin induced oxidative stress by regulating the Keap1-Nrf2-ARE and autophagy signaling pathways. *Psychopharmacology (Berl).*, **240**(5): 1179-1190.

Linders AN, Dias IB, López Fernández T, Tocchetti CG, Bomer N and Van der Meer P (2024). A review of the pathophysiological mechanisms of doxorubicin-induced cardiotoxicity and aging. *NPJ Aging*, **10**(1): 9.

Ma W, Rousseau Z, Slavkovic S, Shen C, Yousef GM and Ni H (2022). Doxorubicin-induced platelet activation and clearance relieved by salvianolic acid compound: novel mechanism and potential therapy for chemotherapy-associated thrombosis and thrombocytopenia. *Pharmaceuticals (Basel)*, **15**(12): 1444.

Maghraby N, El-Baz MA, Hassan A, Abd-Elghaffar SK, Ahmed AS and Sabra MS (2025). Metformin alleviates doxorubicin-induced cardiotoxicity via preserving mitochondrial dynamics balance and calcium homeostasis. *Appl. Biochem. Biotechnol.*, **197**(4), 2713-2733.

Mahdizadeh F, Fazaeli A, Rahimi S, Ojarudi M, Sobhi P, Bahrami M and Rezagholizadeh L (2025). Combined effects of metformin and coenzyme Q10 on doxorubicin-induced cardiotoxicity in male wistar rats. *Sci. Rep.*, **15**(1): 20725.

Meredith AM and Dass CR (2016). Increasing role of the cancer chemotherapeutic doxorubicin in cellular metabolism. *J. Pharm. Pharmacol.*, **68**(6): 729-741.

Mitry MA and Edwards JG (2016). Doxorubicin induced heart failure: Phenotype and molecular mechanisms. *Int. J. Cardiol. Heart. Vasc.*, **10**: 17-24.

Mustafa A, Indiran MA, Shanmugham R and Ramalingam K (2023). Anti-inflammatory activity of lauric acid, thiocolchicoside and thiocolchicoside-lauric acid formulation. *Bioinformation*, **19**(11): 1075.

Naderi Y, Khosraviani S, Nasiri S, Hajiaghaei F, Aali E, Jamialahmadi T, Banach M and Sahebkar A (2023). Cardioprotective effects of minocycline against doxorubicin-induced cardiotoxicity. *Biomed. Pharmacother.*, **158**: 114055.

Nadiah S, Djabir YY, Arsyad MA and Rahmi N (2023). The cardioprotective effect of extra virgin olive oil and virgin coconut oil on isoproterenol-induced myocardial infarction in rats. *Farm*, **71**: 194-204.

Nakajima S and Kunugi H (2020). Lauric acid promotes neuronal maturation mediated by astrocytes in primary cortical cultures. *Heliyon*, **6**(5): e03892.

Namachivayam A and Gopalakrishnan AV (2023). Effect of Lauric acid against ethanol-induced hepatotoxicity by modulating oxidative stress/apoptosis signalling and HNF4α in Wistar albino rats. *Heliyon*, **9**(11): e21267.

Nitbani FO, Tjitda PJP, Nitti F, Jumina J and Detha AIR (2022). Antimicrobial properties of lauric acid and monolaurin in virgin coconut oil: A review. *Chem. Bio. Eng. Reviews*, **9**(5): 442-461.

Nonaka Y, Takagi T, Inai M, Nishimura S, Urashima S, Honda K, Aoyama T and Terada S (2016). Lauric acid stimulates ketone body production in the KT-5 astrocyte cell line. *J. Oleo. Sci.*, **65**(8): 693-699.

Octavia Y, Tocchetti CG, Gabrielson KL, Janssens S, Crijns HJ and Moens AL (2012). Doxorubicin-induced cardiomyopathy: From molecular mechanisms to

therapeutic strategies. *J. Mol. Cell Cardiol.*, **52**(6): 1213-1225.

Pan DS, Li B and Wang SL (2022). Evaluation of biomarkers for doxorubicin-induced cardiac injury in rats. *Exp. Ther. Med.*, **24**(6): 712.

Pecoraro M, Del Pizzo M, Marzocco S, Sorrentino R, Ciccarelli M, Iaccarino G, Pinto A and Popolo A (2016). Inflammatory mediators in a short-time mouse model of doxorubicin-induced cardiotoxicity. *Toxicol. Appl. Pharmacol.*, **293**: 44-52.

Pugazhendhi A, Edison TNJI, Velmurugan BK, Jacob JA and Karuppusamy I (2018). Toxicity of doxorubicin (Dox) to different experimental organ systems. *Life Sci.*, **200**: 26-30.

Sedik AA, Elgohary R, Khalifa E, Khalil WK, I Shafey H, B Shalaby, M SO Gouida M and M Tag Y (2024). Lauric acid attenuates hepato-metabolic complications and molecular alterations in high-fat diet-induced nonalcoholic fatty liver disease in rats. *Toxicol. Mech. Methods.,* **34**(4): 454-467.

Sergazy S, Shulgau Z, Fedotovskikh G, Chulenbayeva L, Nurgozhina A, Nurgaziyev M, Krivyh E, Kamyshanskiy Y, Kushugulova A and Gulyayev A (2020). Cardioprotective effect of grape polyphenol extract against doxorubicin induced cardiotoxicity. *Sci. Rep.*, **10**(1): 14720.

Shaker RA, Abboud SH, Assad HC and Hadi N (2018). Enoxaparin attenuates doxorubicin induced cardiotoxicity in rats via interfering with oxidative stress, inflammation and apoptosis. *BMC Pharmacol. Toxicol.*, **19**: 1-10.

Shi S, Chen Y, Luo Z, Nie G and Dai Y (2023). Role of oxidative stress and inflammation-related signaling pathways in doxorubicin-induced cardiomyopathy. *Cell Commun. Signal*, **21**(1): 61.

Silalahi J, Karo LK, Sinaga SM and Silalahi YCE (2018). Composition of fatty acid and identification of lauric acid position in coconut and palm kernel oils. *IDJPCR.,* **1**(2): 1-8.

Sritharan S and Sivalingam N (2021). A comprehensive review on time-tested anticancer drug doxorubicin. *Life Sci.*, **278**: 119527.

Türkmen M and Koçer O (2021). Variation of components in laurel (*Laurus nobilis L.*) fixed oil extracted by different methods. *Int. J. Chem. Technol.*, **5**(2): 167-171.

Uchiyama M and Mihara M (1978). Determination of malonaldehyde precursor in tissues by thiobarbituric acid test. *Anal. Biochem.,* **86**(1): 271-278.

Warpe VS, Mali VR, Arulmozhi S, Bodhankar SL and Mahadik KR (2015). Cardioprotective effect of ellagic acid on doxorubicin induced cardiotoxicity in wistar rats. *J. Acute. Med.*, **5**(1): 1-8.

Zhang W, Wang X, Tang Y and Huang C (2023). Melatonin alleviates doxorubicin-induced cardiotoxicity via inhibiting oxidative stress, pyroptosis and apoptosis by activating Sirt1/Nrf2 pathway. *Biomed. Pharmacother*, **162**: 114591.

Zhou S, Palmeira CM and Wallace KB (2001). Doxorubicin-induced persistent oxidative stress to cardiac myocytes. *Toxicol. Lett.*, **121**(3): 151-157.